SAND2014-15332C

Measuring Time-Resolved Detonation Velocity Using Wavelet Analysis and Microwave Interferometry

D. E. Kittell, J. O. Mares, and S. F. Son[1]

[1]Purdue University, West Lafayette, Indiana, USA

Abstract

A continuous wavelet transform (CWT) based on the Gabor mother wavelet was used to analyze microwave interferometer data and calculate time-resolved detonation velocity. This technique is compared with established peak-picking and quadrature methods using a combination of real and manufactured data for a small-scale explosives characterization experiment. Further, this approach is expected to have greater flexibility for optimizing time-frequency resolution than the short-time Fourier transform (STFT) alternatives. Results show that the wavelet-based analysis has multiple advantages over both peak-picking and quadrature, including a greater robustness for handling high levels of signal noise (e.g. SNR=3-5), increased velocity-time resolution, and a single tunable parameter – the Gabor wavelet shaping factor (Gs) – that may be optimized for different types of signals. A cost function is proposed to minimize the error in velocity due to Gs, and it is shown to be more reliable than previous methods using Shannon entropy. Overall, the wavelet based technique is suggested as an improved addition to the analysis tools used in the field of explosives research and in particular to microwave interferometry. This analysis approach could also be applied to other experimental data.

Introduction

Microwave interferometry (MI) is an established technique to measure shock and detonation velocities in explosives. This technique is used to measure the phase and amplitude of microwave signals that are transmitted through an unreacted explosive and reflected back at locations of interest. These reflection points are located at dielectric discontinuities such as a shock wave or a reaction front [1,2] that occur in the media during a detonation event. The phase measurements can then be used to infer the relative position and velocity of the phenomena. Despite ongoing research since the early 1950s [3] and subsequent improvements made to interferometers [4-6], the associated data analysis tools have remained largely unchanged over the last 30 years [7,8]. While the established techniques are often adequate for tracking the location of a moving strong reflector as in a shock or detonation wave, instantaneous velocity measurements in less ideal systems remain challenging due to inherent numerical errors associated with these methods. A new approach could be considered to exploit the proportionality of the velocity of the reflector to the relative phase change of the signal through the use of time-frequency analysis. This would suggest consideration of a continuous wavelet transform (CWT) due to greater flexibility for optimizing time-frequency resolution than the

short-time Fourier transform (STFT) alternative [9].due to greater flexibility for optimizing time-frequency resolution than the short-time Fourier transform (STFT) [9].

Difficulties associated with detonation velocity measurements are primarily due to the non-ideality of the signal. Total reflection of the microwave signal is never realized due to partial transmission of the signal through the wave front of interest, as well as attenuation of the signal through absorption and dispersion effects of the explosive media and the reaction front. In addition, real signals may contain several undesirable features related to important physical processes (e.g. damping, abrupt amplitude changes, and multiple dominant frequencies) and experimental realities (e.g. low signal-to-noise ratio). The current techniques attempt to account for these non-idealities at the expense of possibly introducing error through digital filtering, normalization, and smoothing [5] in order to obtain position-time results. Velocity is then numerically derived from position-time data, resulting in higher noise due to the numerical derivative amplification of noise, and consequently there can be loss of subtle transient features. In contrast, a wavelet analysis technique could allow for direct velocity measurement and is well-adapted to transient signals and is more robust in the analysis of real signals without the need of heavy filtering, and may allow for clearer observation of transient events of the wave velocity [10-12].

Wavelet analysis has been applied in similar fields of interferometry [10-15], including photonic Doppler velocimetry (PDV) [10,11] and optical techniques such as velocity interferometer system for any reflector (VISAR) [12]. For these applications, a CWT was shown to be advantageous for measuring shock velocity [10-12]. In this work, a new data analysis technique is proposed to directly measure velocity of a detonation event using a different CWT based method. The proposed technique was compared to currently established procedures by processing manufactured data with known frequency-time content and effective error was evaluated for each method. Select examples of real data of a small scale explosives test were processed using each method and the results are directly compared for further evaluation. This method is suggested as an improved addition to the analysis tools used in the field of microwave interferometry, and possibly other similar data.

Experimental Methods

A 35 GHz signal was generated using a custom microwave interferometer [8] and transmitted to the test article through a solid 0.635 cm dia. polytetrafluoroethylene (PTFE) waveguide. A quadrature mixer was used to produce two-channel output 90 degrees out of phase, and was recorded at 2.5 GHz using a Tektronix DPO4034 Digital Phosphor Oscilloscope. Timing of the experiment is based on first light observed by fiber optics: a M34L02 Thorlab patch cable with a 600 μm core diameter transmitted light to a DET10A Thorlab photodetector with a 1 ns rise time. The detonation is contained inside a thick-walled steel box; a schematic of the experiment is shown in Fig. 3.

In this study, two types of explosives were pressed into 0.651 cm I.D. 304 stainless steel tubes for velocity measurement: Kinepak ammonium nitrate mixed with fuel oil (ANFO) and triaminotrinitrobenzene (TATB) powder. To intimately mix the ANFO, 20 g batches were mixed on a Resodyn (Butte, MT) LabRAM resonant mixer for 5 min at 80% intensity. A Teledyne Risi, Inc. RP-502 detonator was used to initiate a detonation in Primasheet 1000 which transitioned into the test explosive. In these experiments, 1.9 g of ideal explosive (~1.44 g/cm^3) and 2 to 2.5 g of the test explosive were used in each trial. TATB samples were incrementally pressed, whereas the ANFO was loosely packed by hand. Pressing details for select cases discussed in this work are summarized in Table 1.

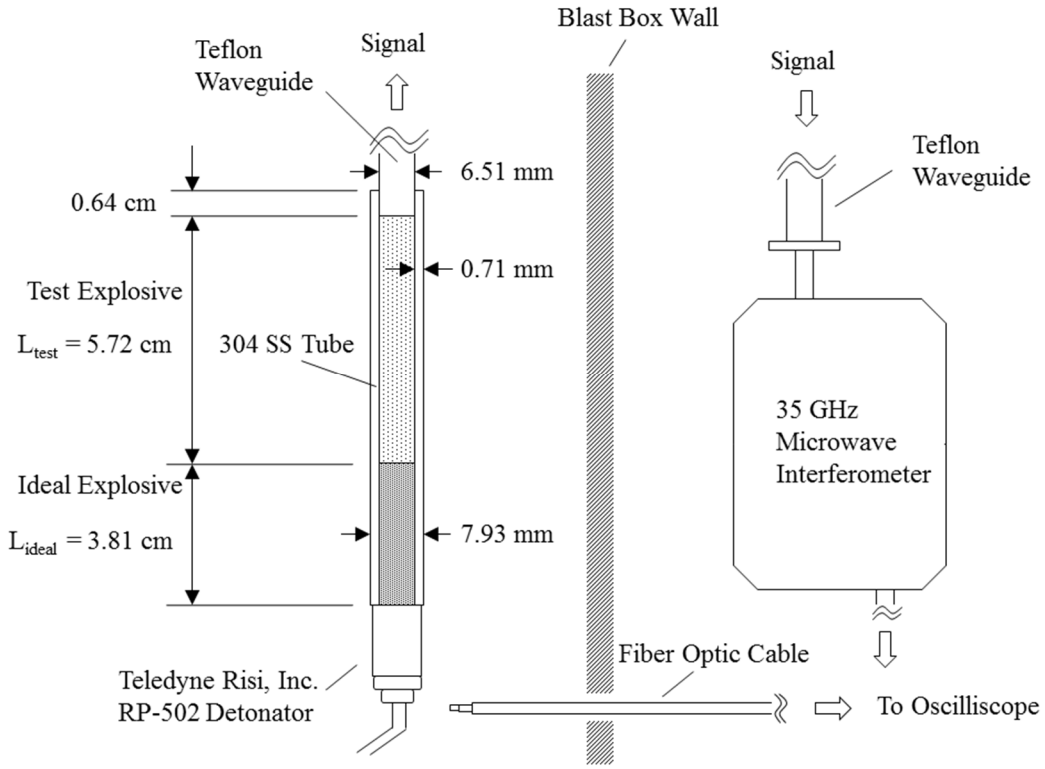

Figure 3. Schematic drawing of the microwave interferometer and test article (not to scale).

Table 1. Pressing details for test cases shown in this work.

Case	Test Explosive	Avg. ρ (g/cm^3)	%TMD	# Increments
T1	ANFO	1.02	60.0	N/A
T2	TATB	1.34	69.3	9x (0.635cm)

The Continuous Wavelet Transform (CWT) Method

Formally, the CWT of a time-varying signal $f(t)$ is given by [16],

$$Wf(u,s) = \int_{-\infty}^{+\infty} f(t)\frac{1}{\sqrt{s}}\psi^*\left(\frac{t-u}{s}\right)dt, \tag{1}$$

where u and s are the translation and scale variables, $\psi(t)$ is the mother wavelet, and ψ^* denotes the complex conjugate. Scale and translation are related to time and frequency through the choice of the mother wavelet. In Eq. (1), the function $\psi(t)$ satisfies the following admissibility condition [16],

$$\int_{-\infty}^{+\infty} \frac{\left|\hat{\psi}(\omega)\right|^2}{|\omega|}d\omega < \infty, \tag{2}$$

where $\hat{\psi}(\omega)$ is the Fourier transform of $\psi(t)$ in frequency space ω. The existence of the integral in Eq. (2) requires a zero mean value for the wavelet [16],

$$\hat{\psi}(0) = 0, \tag{3a}$$

That is,

$$\int_{-\infty}^{+\infty} \psi(t)dt = 0. \tag{3b}$$

Following previous work [9-12], a Gabor mother wavelet was chosen as the basis for the CWT and is given by the formula

$$\psi(t) = \frac{1}{(\sigma^2\pi)^{1/4}}e^{-t^2/2\sigma^2}e^{i\eta t}, \tag{4}$$

where σ and η are the time spread and center frequency parameters. For the Gabor wavelet transform (GWT), time and frequency can be related to scale and translation via [17],

$$t = u, \tag{5a}$$

and

$$\omega = \eta/s. \tag{5b}$$

Kim and Kim [9] show that the Gabor wavelet shape is controlled by a single dimensionless parameter, and introduce the notation of a Gabor wavelet shaping factor $Gs = \sigma\eta$ where σ is set to unity. The shaping factor Gs governs the time-frequency resolution of the GWT according to the relations [18],

$$\sigma_{t_{u,s}} = \frac{Gs}{\sqrt{2}\omega}, \tag{6a}$$

and

$$\sigma_{\omega_{u,s}} = \frac{\omega}{\sqrt{2}Gs}, \tag{6b}$$

where $\sigma_{t_{u,s}}$ and $\sigma_{\omega_{u,s}}$ are the variances (or spread) in time and frequency of the GWT. The effect of Gs on the Gabor wavelet shape is depicted in Fig. 1. The relative weighting on time or frequency resolution is determined by the number of oscillations in the Gabor wavelet shape; in the limit $Gs \to \infty$ the GWT becomes similar to a time-independent FFT. In the limit $Gs \to 0$, the number of oscillations decreases to improve time localization, however this also introduces error due to frequency spreading. When $Gs = 0$, the Gabor wavelet collapses to a normal distribution and violates the admissibility condition (zero mean value). In general, the Gabor wavelet has a non-zero mean; however, it is suggested that $Gs \geq 3$ is sufficient to minimize the mean such that the conditions for a mother wavelet are satisfied [17,19]. Consequently, a frequency bias is introduced near $Gs = 3$ and may be corrected as shown in [20].

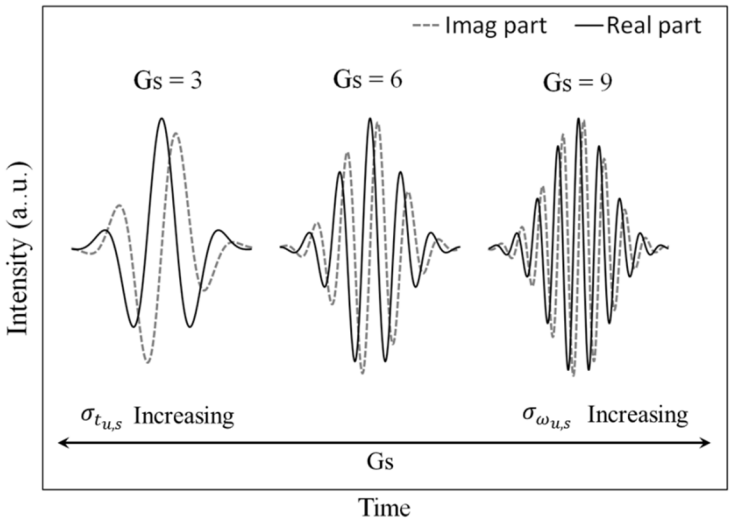

Figure 1. Gabor mother wavelet for shaping factors Gs of 3, 6, and 9.

All CWT-based methods suffer from an edge-effect when part of the wavelet is integrated beyond the length of a signal, using zero-padding or otherwise [18,20,21]. Minimizing the edge-effect is the subject of ongoing research [21]; the approach used in this work was to remove the affected region from the wavelet transform according to

$$R = k\sigma_{t_{u,s}}, \tag{7}$$

where R is the region in time to discard from the start or end, and k is a multiple of the time spread. Values for k are suggested based on the level of signal damping [20].

After the wavelet transform is calculated according to Eq. (1), a normalized scalogram may be used to visualize the time-frequency energy density of the CWT as [17]

$$N_W f(u,s) = \frac{|Wf(u,s)|^2}{s}. \tag{8}$$

Dominant frequencies in the original signal $f(t)$ appear as ridges or peaks on the normalized scalogram. A ridge detection algorithm is used to extract the time-frequency history of the signal [16,22]; in the analysis of a single dominant frequency it is sufficient to consider the location of the maximum scalogram amplitude as a function of time.

Optimization of the Gabor Wavelet Shaping Factor

An optimal Gs value exists to most accurately resolve velocity information from the microwave interferometer signals. The dominant source of calculation error is typically due to insufficient time resolution. The time spread relation of Eq. (6a) may be rearranged to scale Gs

$$\frac{\sigma_{t_{u,s}}}{T} = \frac{Gs}{2\sqrt{2}\pi}, \tag{9}$$

where T is the period at a particular frequency of the signal, and $\sigma_{t_{u,s}}$ is the acceptable time spread. Therefore, to resolve transient phenomena occurring over a time interval on the order of one period Eq. (9) implies that small Gs values $\lesssim 9$ are needed. An optimization scheme is considered to moderate the error in velocity due to frequency resolution within an allowable range for the time spread. Following similar work [17], Gs values were limited between 3-5.5.

Hong and Kim [17,23] recommend an optimization technique for Gs using the Shannon entropy cost function. In one dimension, Shannon entropy is maximized for a constant-valued function and minimized for an impulse (e.g. Dirac delta); this behavior rewards higher levels of signal concentration. In two dimensions, Shannon entropy is used to minimize the time-frequency spreading of the GWT. Shannon entropy-based cost functions require a double summation over time and frequency, therefore a normalization scheme is needed to balance the influence of time and frequency spreading [24]. Hong and Kim [17] favor normalization in time; however, normalization in frequency was also considered here to evaluate the full potential for minimizing the error in velocity.

A new cost function is proposed here using the multi-step process shown in Fig. 2. For a selected *Gs* value, the original signal is analyzed with a GWT to determine the frequency history $\hat{f}(t)$. A reconstructed signal, *y(t)*, is obtained from

$$\theta(t) = 2\pi \int_{t_i}^{t} \hat{f}(\tau) d\tau, \tag{10}$$

and

$$y(t) = Sin\big(\theta(t)\big). \tag{11}$$

A second GWT with the initial Gs value is applied to the reconstructed signal *y(t)* to obtain the frequency history $\tilde{f}(t)$. The two frequency histories are compared using a sum of squared percent errors function (SSPE) given by

$$E = \sqrt{\frac{1}{N}\sum_{i=1}^{N}\left(\hat{f}(t_i)/\tilde{f}(t_i) - 1\right)^2}. \quad (12)$$

The error function is applied to frequency content which does not fall within the region R defined in Eq. (7), and an optimum Gs value is chosen to minimize the estimated error (or actual error if manufactured data is used).

The GWT and frequency integration shown in Eq. (10) are fundamentally different transformations. An optimal Gs value is defined to maximize transformation similarity when they are applied in succession. This cost function is effective for signals having a single dominant time-varying frequency; however, the cost function uniformly weights error across all time and is not well-suited for all signals with mixed transient and steady behavior. Signals having transient events in an otherwise steady frequency should be divided in time to determine the optimal Gs value for isolated parts of the signal. When the frequency history $\tilde{f}(t)$ is known a priori, Eq. (12) may be applied to calculate the true error and true optimum Gs value.

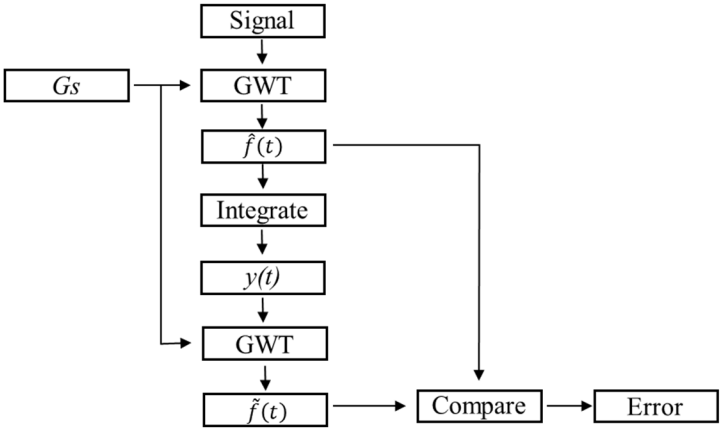

Figure 2. Flow chart for the proposed error function to determine an optimal Gs value.

Data Analysis Procedures

Three analysis techniques – peak-picking, quadrature, and wavelet analysis – were compared between two cases of manufactured data and two cases of real test data summarized in Table 2. All techniques are based on the velocity-frequency relationship [1],

$$v(t) = \frac{\lambda}{2} f(t), \quad (13)$$

where λ is a calibrated material wavelength. The material wavelength depends on microwave frequency, sample diameter, and permittivity – values of λ used in this work are listed in Table 2 from previous studies [8] and theoretical calculations [1,3]. For the peak-picking method, each advance in phase of the signal by 2π corresponds to the advance of the moving reflector by $\lambda/2$

and is indicated by the time of the peaks. Thus, average velocity may be calculated between the i and i+1 peaks according to

$$v_{i+1} = \frac{\lambda/2}{t_{i+1} - t_i}, \tag{14}$$

which is a discretization of Eq. (13). The resolution of this method could be improved using time points from minima, maxima, and zero crossings; however, the most reliable calculations are made between similar features (e.g. peak-to-peak).

Quadrature analysis provides greater spatial resolution than peak-picking and is implemented by replacing Eq. (13) with the set of equations [5]

$$v(t) = \frac{\lambda}{4\pi}\frac{d\theta}{dt}, \tag{15a}$$

and

$$\theta = tan^{-1}\left(\frac{V2}{V1}\right), \tag{15b}$$

where $V1$ and $V2$ are the microwave output signals offset by 90 degrees, and tan^{-1} is the discontinuous arctangent function effectively unwrapping the phase information of the signal. For Eq. (15b) to apply, microwave signals must be normalized between -1 and 1. The signals are filtered in multiple sections, and normalized with a linear mapping between minima and maxima [8]. Filter settings are determined by an FFT of the time signal and experimental judgement; parameters for each test case are summarized in Table 3. For the derivative in Eq. (15a), an FFT-based procedure [25] is used following similar work [8].

Velocity calculations utilizing wavelet analysis are implemented with the MATLAB Wavelet Toolbox™ and a Gabor wavelet (complex Morlet with Fb=2 and Fc=Gs/2π). Microwave signals are de-sampled from 2.5 GHz to 200 MHz, and DC offset is removed. A normalized scalogram is computed from the raw, unfiltered signals; however, a 2D Savitzky-Golay filter [26] is used to eliminate artificial surface roughness on the scalogram that might otherwise disrupt a maximum value search. This filter is first order spanning 33 points in time and frequency. Eq. (5b) is modified to determine the scale-frequency relationship,

$$s = \frac{Fc\ Fs}{f}, \tag{16}$$

where Fs is sampling frequency and f is the signal frequency. Frequency limits of all explosives are shown in Table 2; the frequency range was discretized into 8,000 bins for all cases. A constant time value was subtracted from the edges of the scalogram to remove the edge-effected region (see Table 4). Once the frequency ridge is extracted, velocity is calculated from Eq. (13).

Sharp discontinuities appear in velocity when using Eq. (13) across materials of different wavelengths. One approach for smoothing the velocity across a material interface is to scale the time data of the original signal so that the GWT will numerically compute velocity as a multiple of frequency

$$\hat{t} = \frac{2}{\lambda_i} t, \tag{17}$$

where $\hat{t}$ is the scaled time and λ_i is the material-specific wavelength. The modified signal is re-sampled as this scaling introduces a discontinuous sampling frequency.

Two test cases (M1 and M2) were manufactured in order to compare the velocity obtained from the three analysis methods with a true velocity history. Microwave signals were generated from the frequency histories

$$f(t) = 0.2 + 2.23\, exp(-0.3632\, t), \tag{18}$$

and

$$f(t) = 3.0 + sin(\pi\, t), \tag{19}$$

for cases M1 and M2, where f has units of MHz and t has units of μs. The parameter values in Eqs. (18) and (19) were selected to approximately match real data sets. Eq. (10) is used to calculate $\theta(t)$, and two channel output is simulated with an impedance mismatch [3,5],

$$V1 = A(t)\frac{2r - (r^2+1)\, cos\big(\theta(t)\big)}{1 + r^2 - 2r\, cos\big(\theta(t)\big)}, \tag{20}$$

and

$$V2 = A(t)\frac{2r - (r^2+1)\, sin\big(\theta(t)\big)}{1 + r^2 - 2r\, sin\big(\theta(t)\big)}, \tag{21}$$

where $V1$ and $V2$ are the output channels in mV, $A(t)$ is the signal amplitude, and r is the reflection coefficient (measures departure from a pure sinusoid). The reflection coefficient was introduced to mimic real effects observed in the microwave signals, and was set to 0.05 and 0.3 for M1 and M2, respectively. Constant amplitude was used for M1, but the amplitude for M2 was varied according to

$$A(t) = 1.82\, exp(0.0646\, t). \tag{22}$$

White Gaussian noise was added to each signal and SNR levels are summarized in Table 2.

Table 2. SNR, frequency limits, and wavelength values for all cases.

Case	Type	Explosive	SNR	f_{low} (MHz)	f_{high} (MHz)	$\lambda_{Ex.}$ (mm)
M1	Mfg.	ANFO	3	0.1	2.6	5.12
M2	Mfg.	TATB	15	2.6	3.4	5.06

T1	Test	ANFO	4.4	0.1	2.6	5.12
T2	Test	TATB	16.1	1.8	2.4	5.61
		PS1000		2.3	2.5	5.67

Table 3. Summary of filter parameters needed for the quadrature analysis.

Case	Filter	t_{in} (μs)	t_{out} (μs)	N	Wn
M1	LPF	0	3.5	2	0.008
	LPF	3	7.5	2	0.005
	LPF	6.5	20	2	0.002
	FFTD	all		2	0.008
M2	LPF	0	20	2	0.008
	FFTD	0	20	2	0.004
T1	LPF	0	5.5	2	0.008
	LPF	5	8.5	2	0.005
	LPF	8.5	20	2	0.002
	LPF	8	60	2	0.001
	FFTD	-1.64	4.89	2	0.004
	FFTD	4.89	52.3	2	0.003
T2	LPF	all		2	0.008
	FFTD	-7.68	-2.24	2	0.001
	FFTD	-2.24	7.49	2	0.001

Key: LPF=low pass Butterworth filter of order N, non-dimensional cut-off frequency Wn; FFTD= FFT-based derivative and LPF.

Table 4. Time removed for the edge effect; estimated for Gs=3 and k=3 or k=6 [21].

	LHS		RHS	
Case	k	R (μs)	k	R (μs)
M1	3	-0.5	3	-5.0
M2	6	-1.0	6	-1.0
T1	6	-1.0	3	-5.0
T2	6	-1.0	6	-2.0

Assessment of the Proposed Analysis Approach

I. Manufactured Signals

Two manufactured cases emphasize detonation failure (M1) and unsteady wave motion (M2). These types of transient detonation phenomena are observed in the microwave experiments, and serve to demonstrate the practical application of peak-picking, quadrature, and wavelet analysis. Raw signals offset by 90 degrees are shown below in Fig. 4 and correspond with Eqs. (18) through (22). Signal features such as SNR, amplitude, and impedance mismatch are representative of those obtained from the experimental configuration described in this work.

An optimized Gs value was found using the proposed cost function and compared with the results from Shannon entropy as well as true error. The different functions are plotted against Gs in Fig. 5 and optimum values are summarized in Table 5. The proposed cost function closely matches the shape of the true error. The Shannon entropy is seen to over-predict the optimum Gs value for detonation failure (M1), and fails to predict an optimum Gs value for unsteady wave motion (M2). Pure transient behavior drives the optimum value towards the minimum Gs=3. However, in both cases other minima exist above the range of interest that tune Gs to the steady frequency content of each signal. Additional minima are observed in the proposed cost function for (M2), possibly due to the dual effects of frequency resolution and error introduced near the admissibility condition limit. Overall, the proposed cost function allows one to choose Gs closer to the true optimum value to minimize the error in velocity better than the Shannon entropy functions normalized in either time or frequency.

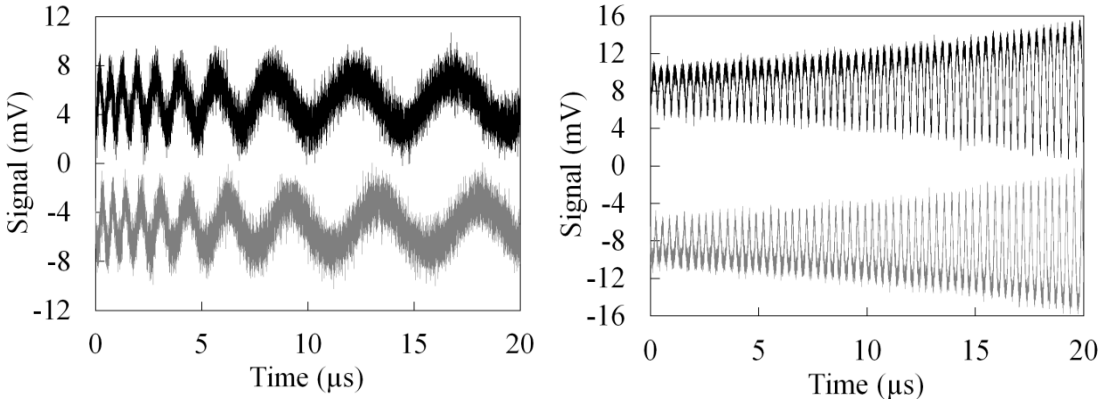

Figure 4. Manufactured signals offset by 90 degrees for detonation failure (case M1, left) and unsteady wave motion (case M2, right).

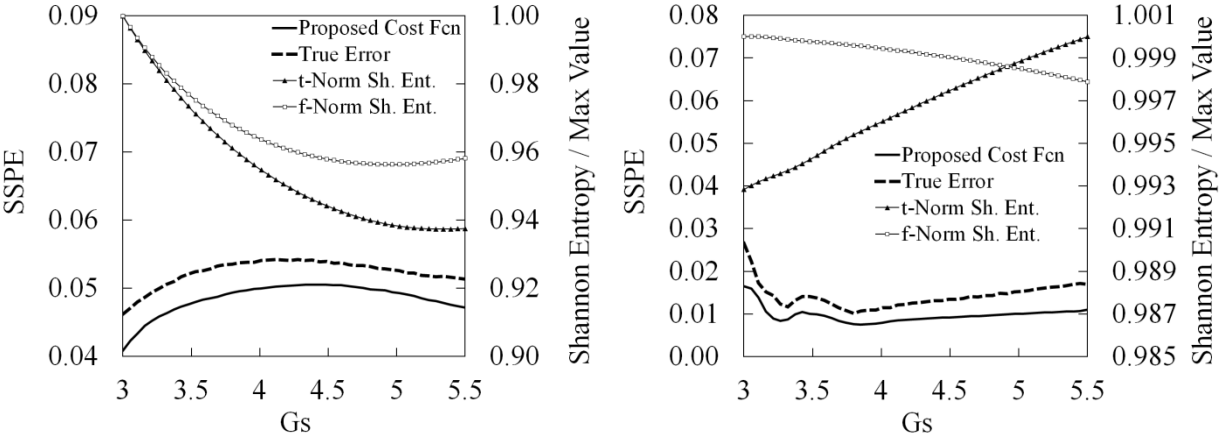

Figure 5. Cost function, Shannon entropy functions, and true error plotted against Gs for manufactured cases M1 (left) and M2 (right).

Table 5. Summary of optimal Gs values for manufactured cases.

Case	Proposed Cost Fcn.	True Error	t-Norm. Sh. Ent.	f-Norm. Sh. Ent.
M1	3.0	3.0	5.3	5.0
M2	3.8	3.8	3.0	>5.5

Peak-picking, quadrature, and wavelet-based velocity calculations for the manufactured cases are shown in Fig. 6. There is a clear advantage in using peak-picking and wavelet analysis over quadrature for detonation failure with a low SNR (M1). Quadrature analysis is based on multiple filter settings, which struggle to distinguish the true signal apart from high levels of white noise. Other difficulties in quadrature for this case may be due to the sharp drop in velocity over 5 μs and lower overall signal frequencies <1 MHz. The visual appearance of the quadrature data for (M1) is similar to recent work [7,8] and justifies the consideration of a new analysis technique such as wavelet analysis.

In the second case showing an unsteady velocity history (M2), all methods – including quadrature – perform well despite added impedance mismatch and noise. A numerical study was conducted to explain the success of quadrature; it was determined that the chosen filter settings were highly effective at analyzing the signal. However, small changes to the period and amplitude of the frequency oscillation were found to compromise the success of the filter settings and the ability for quadrature to analyze this type of data. In addition, velocity is not well matched to the actual velocity history for wavelet and quadrature methods, as clipping is observed in the peak-to-peak value by as much as 0.1 km/s (~10% amplitude decrease). Case M2 is important nonetheless to show that all methods are capable of resolving small oscillations in detonation velocity, and justify the physicality of such oscillations in real test data. From these observations we expect the wavelet analysis to be more robust however with real data.

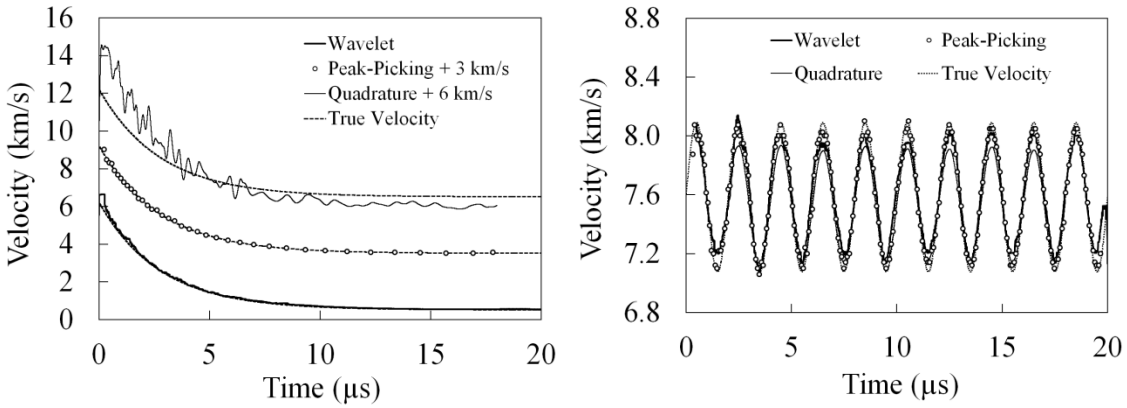

Figure 6. Velocity comparison of peak-picking, quadrature, and wavelet methods for manufactured cases M1 (left) and M2 (right).

II. Real Signals

Two experimental test cases (T1 and T2) were analyzed for detonation failure in ANFO and unsteady detonation velocity in incrementally pressed TATB, respectfully. These cases are representative of the transient detonation phenomena observed in the small-scale characterization experiments. Raw signals offset by 90 degrees are shown below in Fig. 7, and resemble the manufactured data of Fig. 4. Signal indicated before time zero corresponds to an ideal explosive (Primasheet 100) that was used to initiate the test charge. Signal amplitudes vary in both T1 and T2 primarily due to the differences of attenuation in each material, and the strength of the reflection corresponding to detonation or unsupported shock waves. Optimization results for Gs for wavelet cases are shown in Fig. 8 and summarized in Table 6.

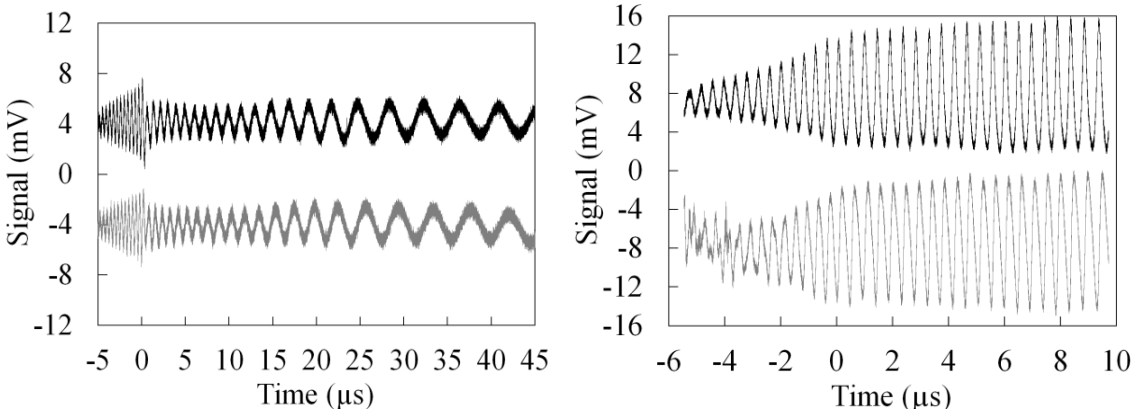

Figure 7. Real quadrature signals (offset by 90 degrees) for detonation failure in ANFO (left) and unsteady wave motion in TATB (right); time zero corresponds to the transition in explosives.

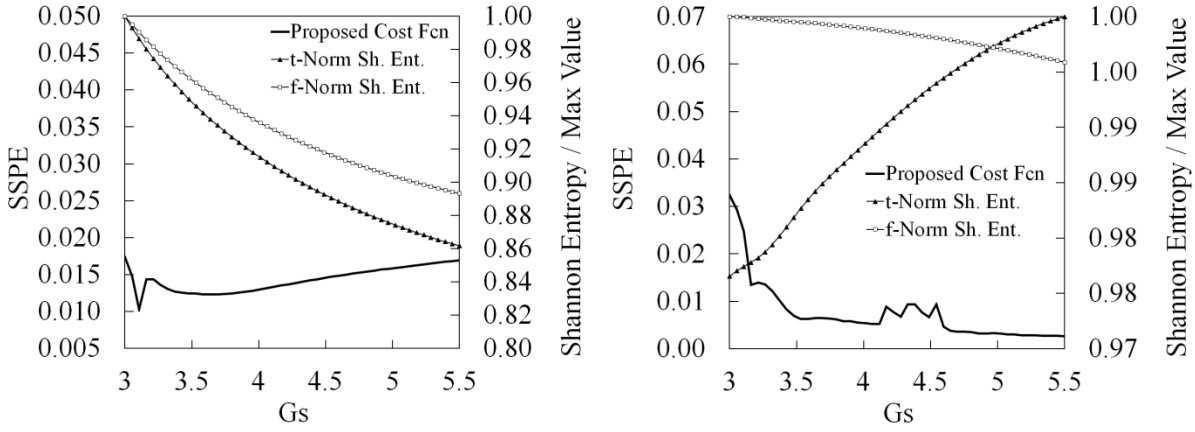

Figure 8. Cost function and Shannon entropy functions plotted against Gs for real test cases *T1* (left) and *T2* (right).

Table 6. Summary of optimal Gs values for real test cases.

Case	Proposed Cost Fcn.	t-Norm. Sh. Ent.	f-Norm. Sh. Ent.
T1	3.1	>5.5	>5.5
T2	4.1	3.0	>5.5

Many similarities are observed in the shape of the cost functions between manufactured and real cases. Trends in Shannon entropy are identical, except for case T1 where the optimum Gs value has moved beyond 5.5. This is likely due to the extended duration of the unsupported shock wave and constant frequency. For case T1, the optimum value in the proposed cost function is near Gs=3 as expected from M1. However, the shape of the proposed cost function for T2 is visually different from M2. Gs values between 3.5-4.1 and a raised section between 4.1-4.6 are thought to be related to the range Gs=3-4 for case M2 (refer back to Fig. 5). As the amplitude of the frequency oscillation about the mean value is slight (~2.1 ± 0.18 MHz), larger Gs values accurately resolve the mean velocity, and the proposed cost function decreases beyond Gs=5.5. The raised section is understood as the range of Gs values where the frequency oscillations begin to be obscured by the mean frequency, therefore an optimum value is selected immediately before, i.e. Gs=4.1.

Velocity results for cases T1 and T2 are shown in Fig. 9. Velocity history before time zero corresponds to the ideal explosive, which shows a nominally steady value of 6.95 km/s. In both cases, similar observations can be made for peak-picking, quadrature, and wavelet analyses. Quadrature analysis is clearly inferior to the peak-picking and wavelet analyses, demonstrating a high susceptibility to noise and loss of subtle transient features. Adjustments to filter coefficients (Table 3) for the quadrature analysis are based on judgement, yet it is found to be impossible to produce velocity plots that are visually similar to the peak-picking and wavelet data. Moreover, the oscillation in velocity for case T2 is obscured by the quadrature analysis yet accentuated with wavelet and peak-picking methods. The oscillation in velocity is real, as evident by the peak-picking method (unaffected from filter aliasing). Physically, it is due to density gradients from an incremental pressing procedure; this was verified by changing the number of pressing increments and observing how the period of the oscillation was affected. Similar density effects have been observed in other work [3].

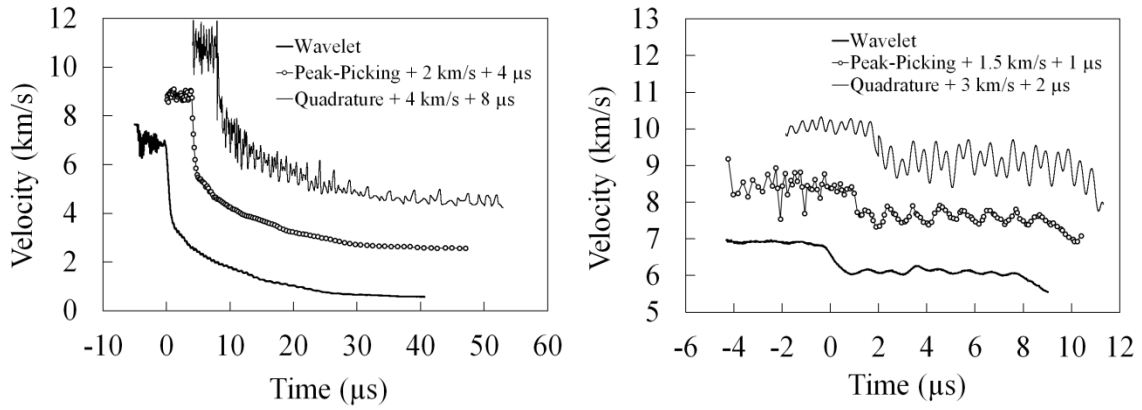

Figure 9. Velocity comparison of peak-picking, quadrature, and wavelet methods for real test cases T1 (left) and T2 (right).

The appearance of wavelet and peak-picking velocity data is similar, and it is necessary to discuss advantages and disadvantages between these two methods. Microwave signals are sampled at 2.5 GHz and collect on the order 10^5 data points per experiment. Only a limited number of those data are used with peak-picking to calculate an average velocity, and thus much of the information contained in the signal is unused (~99.9%). Eq. (9) shows that it is possible with the GWT to resolve information between the peaks of an interference signal; therefore a normalized scalogram processes more time information about the signal. If transient events occur in less time than one period of the interferometer signal, peak-picking cannot resolve velocity or time. The event will simply not be resolved. However, wavelet analysis requires tuning one parameter (Gs) whereas peak-picking is un-biased from signal filtering. An optimization routine for the GWT is critical, especially when investigating subtle transient features in velocity. The suggested value Gs = 5.5 from Shannon entropy completely obscures the oscillation in cases M2 and T2, and distorts the other cases as well. A final observation is that wavelet analysis may clip the full peak-to-peak velocity oscillation in cases M2 and T2, and this is also related to the optimization scheme.

The full advantage of a wavelet-based analysis is the capability to track multiple frequencies in time. For illustration, the single-sided amplitude spectrum is shown for cases M2 and T2 in Fig. 10. Multiple frequency peaks are observed in the signal – it is difficult to selectively filter these peaks for the quadrature analysis. However, it is possible to independently track the location of each of these peaks in time and frequency on a normalized scalogram. This capability will prove advantageous if simultaneous frequencies are observed in the signal, which may potentially occur due to decoupling of the shock and reaction zone. Future work will investigate such an application.

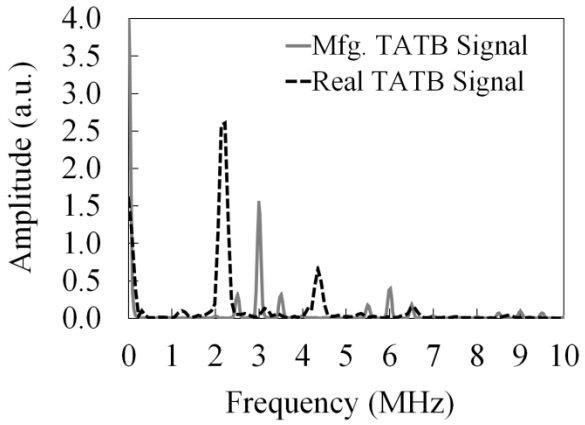

Figure 10. Single-sided amplitude spectrum for case M2 (mfg. TATB signal) and T2 (real TATB signal).

Conclusions

A continuous wavelet transform based on the Gabor mother wavelet was used to analyze microwave interferometer data and calculate time-resolved detonation velocity. This method is suggested as an improved addition to currently established analysis tools. Each method was compared using manufactured and real signals pertaining to a small-scale explosives characterization experiment, and the true error in velocity was determined using manufactured data. From these comparisons, wavelet analysis shows several advantages, including (1) greater robustness for handling noise, (2) increased velocity-time resolution to extract information between peaks in the interference signal, and (3) a single tunable parameter which may be optimized for increased accuracy. Peak-picking and wavelet methods were shown to perform better than quadrature analysis, for which transient features were obscured due to higher sensitivity to signal noise. Oscillations in velocity due to density gradients from an incremental pressing procedure were resolved with peak-picking and wavelet analysis only.

Accurate velocity calculations for the wavelet analysis required an optimization routine to determine a value for the Gabor wavelet shaping factor. Possible values were limited between 3 and 5.5 by the admissibility condition and the acceptable time resolution needed to resolve transient detonation phenomena. A proposed cost function was developed in this work and compared against the Shannon entropy functions used in related work. It was found that the proposed cost function more accurately represents the true velocity history than the Shannon functions, which have difficulty optimizing Gs for transient behavior.

Overall, wavelet analysis is an advanced multi-resolution tool with potential long-term advantages for processing microwave interferometer data. It has been considered over the short-time Fourier transform due to greater flexibility in time-frequency resolution, and has the intriguing potential to more accurately resolve multiple frequencies. This may prove advantageous for studying the decoupling of shock and reaction zones, and should be

investigated in future work. From the results of this work, wavelet analysis should make an improved addition to the fields of microwave interferometry and explosives research, wherever peak-picking and quadrature analysis are currently used to measure a time-resolved velocity.

Acknowledgements

This project was funded by the U.S. Department of Homeland Security under award 2013-ST-061-ED0001 for the awareness and localization of explosives-related threats (ALERT).

References

[1]Krall, A. D., Glancy, B. C., and Sandusky, H. W. "Microwave interferometry of shock waves. I. Unreacting porous media." *J. Appl. Phys.*, **74**(10):6322-6327, 1993.

[2]Glancy, B. C., Sandusky, H. W., and Krall, A. D. "Microwave interferometry of shock waves. II. Reacting porous media." *J. Appl. Phys.*, **74**(10):6328-6334, 1993.

[3]Cawsey, G. F., Farrands, J. L., and Thomas, S. "Observations of detonation in solid explosives by microwave interferometry." *P. Roy. Soc. A-Math Phys.*, **248**(1255):499-521, 1958.

[4]Strand, L. D., Schultz, A. L., and Reedy, G. K. "Microwave Doppler shift technique for determining solid propellant transient regression rates." *J. Spacecraft Rockets*, **11**(2):75-83, 1974.

[5]McCall, G. H., Bongianni, W. L., and Miranda, G. A. "Microwave interferometer for shock wave, detonation, and material motion measurements." *Rev. Sci. Instrum.*, **56**(8):1612-1618, 1985.

[6]Foss, D. T., Roby, R. J., and O'Brien, W. F. "Development of a dual-frequency microwave burn-rate measurement system for solid rocket propellant." *J. Propul. Power*, **9**(4):497-498, 1993.

[7]Bel'skii, V. M., Mikhailov, A. L., Rodinov, A. V., and Sedov, A. A. "Microwave diagnostics of shock-wave and detonation processes." *Combust. Explo. Shock*, **47**(6):639-650, 2011.

[8]Janesheski, R. S., Groven, L. J., and Son, S. F. "Detonation failure characterization of non-ideal explosives." *Propell. Explos. Pyrot.*, Submission 201300041 [under review].

[9]Kim, Y. Y., and Kim, E.-H. "Effectiveness of the continuous wavelet transform in the analysis of some dispersive elastic waves." *J. Acoust. Soc. Am.*, **110**(1):86-94, 2001.

[10]Liu, S., Wang, D., Li, T., Chen, G., Li, Z., and Peng, Q. "Analysis of photonic Doppler velocimetry data based on the continuous wavelet transform." *Rev. Sci. Instrum.*, **82**(2):023103, 2011.

[11]Song, H., Wu, X., Huang, C., Wei, Y., and Wang, X. "Measurement of fast-changing low velocities by photonic Doppler velocimetry." *Rev. Sci. Instrum.*, **83**(7):073301, 2012.

[12]Sur, A., Rav, A. S., Pandey, G., Joshi, K. D., and Gupta, S. C. "Analysis of velocimetry data based on continuous wavelet transform: application to shock wave physics experiments." *Advanced Electronic Systems (ICAES), IEEE International Conference on*, pp. 147-151, 2013.

[13]Fu, Y., Tay, C. J., Quan, C., and Miao, H. "Wavelet analysis of speckle patterns with a temporal carrier." *Appl. Optics*, **44**(6):959-965, 2005.

[14]Ferretti, A., Prati, C., and Rocca, F. "Permanent scatters in SAR interferometry." *IEEE T. Geo. Sci. Remote*, **39**(1):8-20, 2001.

[15]Bruskin, L. G., Mase, A., Tokuzawa, T., Oyama, N., Itakura, A., and Tamano, T. "Measurement of plasma density using wavelet analysis of microwave reflectometer signal." *Rev. Sci. Instrum.*, **69**(2):425-430, 1998.

[16]Mallat, S., A Wavelet Tour of Signal Processing, 2nd edition, Academic Press, New York, 1999.

[17]Hong, J.-C., and Kim, Y. Y. "Determination of the optimal gabor wavelet shape for the best time-frequency localization using the entropy concept." *Exp. Mech.*, **44**(4):387-395, 2004.

[18]Simonovski, I., and Boltežar, M. "The norms and variances of the Gabor, Morlet and general harmonic wavelet functions." *J. Sound Vib.*, **264**(3):545-557, 2003.

[19]Deng, Y. Q., Wang, C., Chai, L., and Zhang, Z. "Determination of gabor wavelet shaping factor for accurate phase retrieval with wavelet-transform." *Appl. Phys. B-Lasers O.*, **81**(8):1107-1111, 2005.

[20]Slavič, J., Simonovski, M., and Boltežar, M. "Damping identification using a continuous wavelet transform: application to real data." *J. Sound Vib.*, **262**(2):291-307, 2003.

[21]Boltežar, M., and Slavič, J. "Enhancements to the continuous wavelet transform for damping identifications on short signals." *Mech. Syst. Signal Pr.*, **18**(5):1065-1076, 2004.

[22]Delprat, N., Escudié, B., Guillemain, P., Martinet, R. K., Tchamitchian, P., and Torrésani, B. "Asymptotic wavelet and gabor analysis: extraction of instantaneous frequencies." *IEEE T. Inform. Theory*, **38**(2):644-664, 1992.

[23]Hong, J.-C., Sun, K. H., and Kim, Y. Y., "Dispersion-based short-time Fourier transform applied to dispersive wave analysis." *J. Acoust. Soc. Am.*, **117**(5):2949-2960, 2005.

[24]Coifman, R. R., and Wickerhauser, M. V. "Entropy-based algorithms for best basis selection." *IEEE T. Inform. Theory*, **38**(2):713-718, 1992.

[25]De Levie, R., Sarangapani, S., and Czekaj, P., "Numerical differentiation by Fourier transform as applied to electrochemical interfacial tension data." *Anal. Chem.*, **50**(1):110-115, 1978.

[26]Savitzky, A., and Golay, M. J. "Smoothing and differentiation of data by simplified least squares procedures." *Anal. Chem.*, **36**(8):1627-1639, 1964.